# Identification of the anti-diffusion coefficient for the linear Kuramoto-Sivashinsky equation

Diego Gajardo, Alberto Mercado, Juan Carlos Muñoz

# Identification of the anti-diffusion coefficient for the linear Kuramoto-Sivashinsky equation

Diego Gajardo,* Alberto Mercado † and Juan Carlos Muñoz ‡

October 5, 2020

**Abstract**

The Kuramoto-Sivashinsky equation is a fourth-order partial differential equation used as a model for physical phenomena such as plane flame propagation and phase of turbulence. The inverse problem of recovering the second-order coefficient from the knowledge of the solution in final time, for the linear version of the equation, is studied in this article. The inverse problem is formulated as a regularized nonlinear optimization problem, from which the local uniqueness and the stability are proved. Finally, an algorithm for the reconstruction of the coefficient is proposed and several numerical simulations are presented.

**Keywords:** Kuramoto-Sivashinsky equation, inverse problem, non-linear PDE optimization.

## 1 Introduction

The Kuramoto-Sivashinsky equation is the fourth-order non-linear parabolic equation

$$u_t + u_{xxxx} + \gamma u_{xx} + uu_x = f, \tag{1}$$

where $\gamma > 0$ is known as the anti-difussion parameter. This equation was derived independently by Kuramoto and Tsuzuki [15] and by Sivashinsky [26], as a model for phase of turbulence in reaction-diffusion systems and for the physical phenomena of plane flame propagation, respectively.

In this article, we consider the linear Kuramoto-Sivashinsky (KS) equation with non-constant coefficients $\sigma = \sigma(x)$ for the diffusion and $\gamma = \gamma(x)$ for the anti-diffusion. For $L, T > 0$, this system is given by

$$\begin{cases} u_t + (\sigma(x)u_{xx})_{xx} + \gamma(x)u_{xx} = f, & (x,t) \in (0,L) \times (0,T), \\ u(0,t) = 0, \quad u(L,t) = 0, & t \in (0,T), \\ u_x(0,t) = 0, \quad u_x(L,t) = 0, & t \in (0,T), \\ u(x,0) = u_0(x), & x \in (0,L), \end{cases} \tag{2}$$

*Departamento de Matemática, Universidad Técnica Federico Santa María, Casilla 110-V, Valparaíso, Chile (diego.gajardom@alumnos.usm.cl).

†Departamento de Matemática, Universidad Técnica Federico Santa María, Casilla 110-V, Valparaíso, Chile and Institut de Mathématiques de Toulouse, UMR 5219, France. (alberto.mercado@usm.cl) Partial support of projects FONDECYT 1171712, BASAL Project CMM - U. de Chile and Labex CIMI (Centre International de Mathématiques et d'Informatique), ANR-11-LABX-0040-CIMI, within the program ANR-11-IDEX-0002-02.

‡Departamento de Matemáticas, Universidad del Valle, Calle 13 No. 100-00, Cali, Colombia (juan.munoz@correounivalle.edu.co). Supported by the projects MATH-AmSud-Colciencias C.I. 71020 and Colciencias 1106-712-50006, C.I. 71045.

where $f$ and $u_0$ are the given source term and initial condition, respectively.

This work is concerned with the inverse problem of retrieving the anti-diffusion coefficient $\gamma = \gamma(x)$ in the KS equation (2), from the observation of the solution in final time $u(\cdot, T)$ in $(0, L)$. The role of the anti-diffusion coefficient in the stability properties of the non-linear KS equation with constant coefficients is well-known (see [16]). Hence, methods for recovering this parameter can be useful in getting information about the instability of the system.

Several kinds of inverse problems for partial differential equations has been widely studied in the literature. For related problems, we can cite [13], [23] and [24], where inverse problems of recovering a source term or a coefficient in the cantilevered beam equation and the linear Korteweg-de Vries (KdV) equation are studied using optimization methods, and [21], where the identification of the linear velocity coefficient in a scalar dispersive Benjamin-Bona-Mahony equation is considered. Concerning inverse problems for the linear Kuramoto-Sivashinsky equation, in [4] and [12], Carleman estimates are used to obtain Lipschitz stability of the inverse problem of recovering coefficients of the equation, from knowledge of traces of the solution at one end of the interval, given by $u_{xx}(0, \cdot)$ and $u_{xxx}(0, \cdot)$ on $(0, T)$, and also a measurement of the solution in a given positive time in the whole domain. The article [11] studies the case of internal measurements given by $u$ and $u_t$ in $\omega \times (0, T)$, in addition to the derivatives of the solution in some positive time. In this article we follow a more realistic approach, by means of only considering the measurement of the solution in a given final time $T > 0$. As far we know, there are no results in the literature concerning inverse problems and numerical identification of the anti-diffusion coefficient of the non-linear KS equation, and we intend that this work can serve as a first step in that direction.

We propose an optimization-based approach for reconstructing $\gamma$ given the final time measurement $m \in L^2(0, L)$. For a coefficient $\gamma \in H^1(0, L)$, the unique weak solution of (2), denoted by $u(\gamma)$, belongs to $C([0, T]; L^2(0, L))$ (see Theorem 1.1), and thus it makes sense to consider the functional given by

$$J(\gamma) := \frac{1}{2}\|u(\cdot, T; \gamma) - m\|_{L^2}^2 + \frac{\alpha}{2}\|\gamma\|_{H^1}^2, \tag{3}$$

where $\alpha > 0$. We consider the minimization problem

$$\min_{\gamma \in \mathcal{M}} J(\gamma), \tag{4}$$

where the admissible set $\mathcal{M}$ is defined by

$$\mathcal{M} := \{\gamma \in H^1(0, L) : \|\gamma\|_{H^1} \leq \eta\},$$

for some $\eta > 0$.

The main result of this work is the following.

**Theorem 1.1.** *Given $m$ and $\widetilde{m} \in L^2(0, L)$, let $\gamma$ and $\widetilde{\gamma} \in \mathcal{M}$ be solutions of the optimization problem (4), respectively. Then, there exists $T_0 > 0$ and a positive constant $K$ independent of $T$ such that for all $T \in (0, T_0)$,*

$$\|\gamma - \widetilde{\gamma}\|_{H^1} \leq K\|m - \widetilde{m}\|_{L^2}. \tag{5}$$

From this stability result, we directly obtain the uniqueness of the solution of the optimization problem (4):

**Corollary 1.1.** *Assume that the hypothesis of Theorem 1.1 hold. If $m = \widetilde{m}$, then we have that there exists $T_0 > 0$ such that for all $T \in (0, T_0)$, $\gamma = \widetilde{\gamma}$.*

Besides, we illustrate numerically the solution of the inverse problem considered for the KS equation by approximating the solution of the optimization-based approach given in (4) for the reconstruction of the anti-diffusion parameter and present some numerical experiments. The minimization of the objective functional constrained by the KS equation is performed by using the iterative L-BFGS-B algorithm, described for instance by Byrd et al. [5], and Zhu et al. [27]. The spatial discretization of both the forward and adjoint problem is developed with the Finite Element Method (FEM), and the corresponding time stepping is carried out by means of an implicit two-step leap-frog type strategy, which guarantees the required numerical stability. We found that selecting appropriately the regularization term in the functional $J(\gamma)$ and the final time $T$, we can obtain a good reconstruction of the parameter, even in the presence of noise in the final measurement. The stability result established in Theorem 1.1 is also validated by using the numerical scheme proposed.

The remainder of this paper is organized as follows. In section 2, we prove the existence of a unique weak solution for the KS equation (2). Next, in section 3 we formulate the inverse problem as a non-linear optimization problem and we show the local uniqueness and stability. In section 4, we propose an algorithm for the reconstruction of the parameter and present some numerical simulations. In the final section, we present some conclusions and future works related to the contents of this paper.

**Notation.** If there is no danger of confusion, we write $L^p$ instead of $L^p(0,L)$, and analogously $H^k$ instead $H^k(0,L)$ for Sobolev spaces. The corresponding spaces of functions with zero traces get an additional index 0. Further, $\langle\cdot,\cdot\rangle$ is the duality product between $H^{-2} := (H_0^2)'$ and $H_0^2$ and $(\cdot,\cdot)$ is the scalar product of $L^2$. We identify $L^2$ with its dual space such that we typically work in the Gelfand triple $H_0^2 \subset L^2 \subset H^{-2}$.

# 2 Well-posedness of the direct problem

This section is devoted to the proof of well-posedness of system (2). More precisely, we prove that system (2) has a unique weak solution by using Galerkin's method (see, e.g. [8]).

First, we consider the following definition.

**Definition 2.1.** *Let $\sigma \in L^\infty(0,L)$ be such that $\sigma(x) \geq \sigma_0$ for a.e. $x \in (0,L)$, $\gamma \in L^\infty(0,L)$, $f \in L^2(0,T;L^2(0,L))$ and $u_0 \in L^2(0,L)$. We say that $u$ is a weak solution of (2) if $u \in L^2(0,T;H_0^2(0,L))$, $u_t \in L^2(0,T;H^{-2}(0,L))$, $u(\cdot,0) = u_0$ and*

$$\langle u_t(\cdot,t),\varphi\rangle + \int_0^L \sigma(x)u_{xx}\varphi_{xx}dx + \int_0^L \gamma(x)u_{xx}\varphi dx = (f(\cdot,t),\varphi) \text{ a.e. on } (0,T) \tag{6}$$

*for all $\varphi \in H_0^2(0,L)$.*

**Remark 2.1.** *In the previous definition, the condition $u(\cdot,0) = u_0$ is well defined because if $u \in L^2(0,T;H_0^2)$ and $u_t \in L^2(0,T;H^{-2})$, in particular we have that $u \in C([0,T];L^2)$.*

If we set

$$a : [0,T] \times H_0^2 \times H_0^2 \to \mathbb{R}, \;\; a(t,u,w) := \int_0^L (\sigma(x)u_{xx}w_{xx} + \gamma(x)u_{xx}w)dx,$$

the weak formulation (6) is equivalent to

$$\langle u_t(\cdot,t),\varphi\rangle + a(t,u(\cdot,t),\varphi) = (f(\cdot,t),\varphi) \quad \text{for a.e. } t \in (0,T), \tag{7}$$

for all $\varphi \in H_0^2$. In order to prove that there exists a unique weak solution, we proceed by Galerkin approximation in finite-dimensional subspaces of $H_0^2$. To this end, choose some orthogonal basis $(w_j)_{j\in\mathbb{N}}$ of $H_0^2$ that is at the same time an orthonormal basis of $L^2$.

For a positive integer $N$ we define $E_N := span\{w_1, \dots, w_N\}$. We will look for a function $u^N : [0,T] \to H_0^2$ of the form

$$u^N(t) := \sum_{j=1}^{N} c_{N,j}(t) w_j, \tag{8}$$

where the coefficients $c_{N,j}(t)$ $(0 \le t \le T, j = 1, \dots, N)$ satisfies

$$c_{N,j}(0) = (u_0, w_j) \ \ (j = 1, \dots, N), \tag{9}$$

and

$$\langle u_t^N(t), w_j \rangle + a(t, u^N(t), w_j) = (f(\cdot,t), w_j) \quad (0 \le t \le T, \ j = 1, \dots, N). \tag{10}$$

**Lemma 2.1.** *For each $N \in \mathbb{N}$ there exists a unique function $u^N$ of the form (8) satisfying (9) and (10).*

*Proof.* Assuming $u^N$ satisfies (7), we note that

$$\langle u_t^N(t), w_j \rangle = c'_{N,j}(t) \ \ (0 \le t \le T, j = 1, \dots, N).$$

Additionally,

$$a(t, u^N(t), w_j) = \sum_{k=1}^{N} a^{jk}(t) c_{N,k}(t),$$

where $a^{jk}(t) = a(t, w_j, w_k)$ $(j,k = 1, \dots, N)$. If we write $f^j(\cdot,t) = (f(\cdot,t), w_j)$ $(j = 1, \dots, N)$, then (7) becomes the linear system of ODE

$$c'_{N,j}(t) + \sum_{k=1}^{N} a^{jk}(t) c_{N,k}(t) = f^j(\cdot,t) \quad (j = 1, \dots, N), \tag{11}$$

subject to the initial condition (9). From standard theory for ordinary differential equations it follows that there exists a unique absolutely continuous function $c_N = (c_{N,1}(t), \dots, c_{N,N}(t))$ satisfying (9) and (11) for *a.e.* $0 \le t \le T$. Then, $u^N$ defined in (8) solves (10) for a.e. $0 \le t \le T$. □

**Lemma 2.2.** *There exists a constant $C = C(T, \sigma_0, \gamma)$, such that for all $N \in \mathbb{N}$, the solution $u^N$ of (10) satisfies*

$$\|u^N\|_{L^\infty(0,T;L^2)} + \|u^N\|_{L^2(0,T;H_0^2)} + \|u_t^N\|_{L^2(0,T;H^{-2})} \le C \left( \|u_0\|_{L^2} + \|f\|_{L^2(0,T;L^2)} \right). \tag{12}$$

*Proof.* Multiply equation (10) by $c_{N,k}(t)$ and then sum for $k = 1, \dots, N$, we obtain

$$\langle u_t^N, u^N \rangle + a(t, u^N, u^N) = (f, u^N) \ \text{ for a.e. } 0 \le t \le T. \tag{13}$$

The last line is equivalent to write

$$\frac{1}{2} \frac{d}{dt} \|u^N(t)\|_{L^2}^2 + \int_0^L \sigma(x) |u_{xx}^N(t)|^2 dx = - \int_0^L \gamma(x) u_{xx}^N(t) u^N(t) dx + (f(\cdot,t), u^N(t)). \tag{14}$$

If in this equality we consider

$$\begin{aligned} - \int_0^L \gamma(x) u^N(t) u_{xx}^N(t) dx + (f(\cdot,t), u^N(t)) \le \frac{\|\gamma\|_{L^\infty}^2}{2\sigma_0} \|u^N(t)\|_{L^2}^2 + \frac{1}{2} \int_0^L \sigma(x) |u_{xx}^N(t)|^2 dx \\ + \frac{1}{2} \|f(\cdot,t)\|_{L^2}^2 + \frac{1}{2} \|u^N(t)\|_{L^2}^2, \end{aligned}$$

then,

$$\frac{d}{dt}\|u^N(t)\|_{L^2}^2 + \int_0^L \sigma(x)|u_{xx}^N(t)|^2 dx \leq \left(\frac{\|\gamma\|_{L^\infty}^2}{\sigma_0} + 1\right)\|u^N(t)\|_{L^2}^2 + \|f(\cdot,t)\|_{L^2}^2. \tag{15}$$

Gronwall's inequality allows us to conclude from (15) that

$$\begin{aligned}\|u^N(t)\|_{L^2}^2 &\leq \exp\left[T\left(\frac{\|\gamma\|_{L^\infty}^2}{\sigma_0} + 1\right)\right]\left(\|u^N(0)\|_{L^2}^2 + \|f\|_{L^2(0,T;L^2)}^2\right) \\ &\leq \exp\left[T\left(\frac{\|\gamma\|_{L^\infty}^2}{\sigma_0} + 1\right)\right]\left(\|u_0\|_{L^2}^2 + \|f\|_{L^2(0,T;L^2)}^2\right).\end{aligned} \tag{16}$$

Then, (15) is integrated over $(0,T)$ and $\sigma(x) \geq \sigma_0$ a.e. $x \in (0,L)$ is used to get

$$\|u^N(t)\|_{L^2(0,T;H_0^2)}^2 \leq \frac{KT}{\sigma_0}\|u^N(t)\|_{L^2}^2 + \|f(\cdot,t)\|_{L^2}^2 + \|u_0\|_{L^2}^2. \tag{17}$$

To estimate the term $\|u^N(t)\|_{L^2}^2$ in (17) we use (16). Thus we obtain

$$\|u^N(t)\|_{L^2(0,T;H_0^2)}^2 \leq \left(\frac{KT}{\sigma_0}\exp(KT) + 1\right)\left(\|u_0\|_{L^2}^2 + \|f\|_{L^2(0,T;L^2)}^2\right), \tag{18}$$

where

$$K = \frac{\|\gamma\|_{L^\infty}^2}{\sigma_0} + 1.$$

Therefore, combining (16) and (18) leads us to

$$\|u^N\|_{L^\infty(0,T;L^2)}^2 + \|u^N\|_{L^2(0,T;H_0^2)}^2 \leq C\left(\|u_0\|_{L^2}^2 + \|f\|_{L^2(0,T;L^2)}^2\right). \tag{19}$$

To obtain $H^{-2}$ bounds for $u_t^N$, let us finally choose any $\varphi \in H_0^2$ with $\varphi = \varphi^1 + \varphi^2$, where $\varphi^1 \in E_N$ and $\varphi^2 \in E_N^\perp$. Note that $\|\varphi^1\|_{H_0^2} \leq \|\varphi\|_{H_0^2}$. Then,

$$\langle u_t^N(t), \varphi\rangle = \int_0^L u_t^N(t)\varphi^1 dx = (f(\cdot,t),\varphi^1) - a(t,u^N(t),\varphi^1), \tag{20}$$

Using the Schwarz and Poincaré inequalities, we infer that

$$\begin{aligned}(u_t^N(t),\varphi) &\leq \|f(\cdot,t)\|_{L^2}\|\varphi^1\|_{L^2} + \|\sigma\|_{L^\infty}\|u^N(t)\|_{H_0^2}\|\varphi^1\|_{H_0^2} + \|\gamma\|_{L^\infty}\|u^N(t)\|_{H_0^2}\|\varphi^1\|_{L^2} \\ &\leq C_p\|f(\cdot,t)\|_{L^2}\|\varphi^1\|_{H_0^2} + \|\sigma\|_{L^\infty}\|u^N(t)\|_{H_0^2}\|\varphi^1\|_{H_0^2} + C_p\|\gamma\|_{L^\infty}\|u^N(t)\|_{H_0^2}\|\varphi^1\|_{H_0^2} \\ &\leq C(\|u^N(t)\|_{H_0^2} + \|f(\cdot,t)\|_{L^2})\|\varphi^1\|_{H_0^2} \\ &\leq C(\|u^N(t)\|_{H_0^2} + \|f(\cdot,t)\|_{L^2})\|\varphi\|_{H_0^2},\end{aligned} \tag{21}$$

where $C_p$ denote the Poincaré constant and $C$ a constant depending only on $\sigma, \gamma$ and $C_p$. From the last inequality it follows that

$$\|u_t^N(t)\|_{H^{-2}}^2 \leq C\left(\|u_N(t)\|_{H_0^2}^2 + \|f(\cdot,t)\|_{L^2}^2\right). \tag{22}$$

After integrate over $(0,T)$ in (22) and then use (18), we get

$$\begin{aligned}\|u_t^N\|_{L^2(0,T;H^{-2})}^2 &\leq C\left(\int_0^T \|u_N(t)\|_{H_0^2}^2 dt + \int_0^T \|f(\cdot,t)\|_{L^2}^2 dt\right) \\ &\leq C\left(\|u_0\|_{L^2}^2 + \|f\|_{L^2(0,T;L^2)}^2\right).\end{aligned} \tag{23}$$

Finally, combining (19) and (23) we obtain (12). □

**Theorem 2.1.** *Let $\sigma_0 > 0$ and $\sigma \in L^\infty(0,L)$ be such that $\sigma(x) \geq \sigma_0$ a.e. $x \in (0,L)$. Let $\gamma \in L^\infty(0,L)$, $f \in L^2(0,T;L^2(0,L))$ and $u_0 \in L^2(0,L)$. Then, there exists a unique weak solution*

$$u \in C([0,T];L^2(0,L)) \cap L^2(0,T;H_0^2(0,L))$$

*of (2) with $u_t \in L^2(0,T;H^{-2}(0,L))$. Moreover, there exists a constant $C = C(T,\sigma_0,\gamma) \geq 0$ such that*

$$\|u\|_{L^\infty(0,T;L^2)} + \|u\|_{L^2(0,T;H_0^2)} + \|u_t\|_{L^2(0,T;H^{-2})} \leq C\left(\|u_0\|_{L^2} + \|f\|_{L^2(0,T;L^2)}\right). \tag{24}$$

*Proof.* According to Lemma 2.2, we see that sequence $(u^N)_{N\in\mathbb{N}}$ is bounded in $L^2(0,T;H_0^2)$, and $(u_t^N)_{N\in\mathbb{N}}$ is bounded in $L^2(0,T;H^{-2})$. Then, there exists a subsequence of $(u^N)_{N\in\mathbb{N}}$, which for simplicity we still denote by $(u^N)_{N\in\mathbb{N}}$, and a function $u \in L^2(0,T;H_0^2)$ and $u_t \in L^2(0,T;H^{-2})$, such that

$$u^N \to u \text{ weakly in } L^2(0,T;H_0^2), \qquad u_t^N \to u_t \text{ weakly in } L^2(0,T;H^{-2}). \tag{25}$$

Let $\phi \in C_0^\infty(0,T)$ and $w \in E_M$ for some fixed $M \in \mathbb{N}$. Considering $\varphi = \phi(t)w$ in (11) and then integrating over $(0,T)$, we get that for $N \geq M$

$$\int_0^T \langle u_t^N, \phi w\rangle dt + \int_0^T a(t,u^N,\phi w)dt = \int_0^T (f,\phi w)dt.$$

Since $\varphi \in L^2(0,T;H_0^2)$, from (25) we deduce that when $N \to \infty$,

$$\int_0^T \phi\left(\langle u_t, w\rangle + a(t,u,w) - (f,w)\right)dt = 0.$$

From this last identity and the density of $C_0^\infty(0,T)$ in $L^2(0,T)$, we obtain

$$\langle u_t, w\rangle + a(t,u,w) = (f,w) \text{ a.e. } t \in (0,T).$$

Moreover, since $\cup_{M\in\mathbb{N}} E_M$ is dense in $H_0^2$, the last identity hold for every $w \in H_0^2$, and therefore $u$ satisfies (6).
Now we will prove that $u(0) = u_0$. We consider $\phi \in C^\infty([0,T])$ such that $\phi(0) = 1$ and $\phi(T) = 0$. Given $w \in E_M$ we set $\varphi = \phi(t)w$. Through integrating by parts over $(0,T)$, we obtain that

$$(u(0),w) = -\int_0^T \langle u,w\rangle\phi_t dx + \int_0^T a(t,u,w)\phi dt - \int_0^T (f,w)\phi dt. \tag{26}$$

By using a similar argument we have that for Galerkin approximation with $w \in E_M$ and $N \geq M$, we get that

$$(u^N(0),w) = -\int_0^T \langle u^N,w\rangle\phi_t dt + \int_0^T a(t,u^N,w)\phi dt - \int_0^T (f,w)dt.$$

Taking the limit when $N \to \infty$ in the last identity we obtain that

$$(u_0,w) = -\int_0^T \langle u,w\rangle\phi_t dt + \int_0^T a(t,u,w)\phi dt - \int_0^T (f,w)dt. \tag{27}$$

Comparing (26) and (27) we find that

$$(u(0),w) = (u_0,w) \ \ \forall w \in E_M,$$

from which we can deduce that $u(0) = u_0$.
Now, we will prove uniqueness. Let $u$ and $\widetilde{u}$ be weak solutions of (2). We set $y = u - \widetilde{u}$ and we note that by linearity of (2), $y$ solves the following equation:

$$\langle y_t, \varphi\rangle + a(t, y, \varphi) = 0 \text{ for all } \varphi \in H_0^2 \text{ and a.e. } t \in (0, T) \text{ and } y(0) = 0.$$

Taking $\varphi = y$ as a test function in the last equation we get

$$\frac{1}{2}\frac{d}{dt}\|y(t)\|_{L^2}^2 + \int_0^L \sigma(x)|y_{xx}(t)|^2 dx = -\int_0^L \gamma(x) y_{xx}(t) y(t) dx,$$

a.e. $t \in (0, T)$ and $y(0) = 0$. Estimating the right side in the last identity we arrive at

$$\frac{d}{dt}\|y(t)\|_{L^2}^2 + \int_0^L \sigma(x)|y_{xx}(t)|^2 dx \leq \frac{\|\gamma\|_{L^\infty}^2}{\sigma_0}\|y(t)\|_{L^2}^2,$$

and then

$$\frac{d}{dt}\|y(t)\|_{L^2}^2 \leq \frac{\|\gamma\|_{L^\infty}^2}{\sigma_0}\|y(t)\|_{L^2}^2.$$

Since $y(0) = 0$, Gronwall's inequality implies that $y \equiv 0$ and then $u = \widetilde{u}$.
Finally, the estimate (24) can be shown by using the same arguments used in Lemma 2.2. □

# 3 Inverse problem

In this section we show the stability result for the minimization problem (4). First, in the subsection 3.1 we prove the existence of solutions of (4), and then in the subsection 3.2 we deduce the first-order necessary conditions. Finally, using the optimality conditions and energy estimates we prove the local stability result.

## 3.1 Existence of a minimizer

In the following theorem we establish the existence of a minimizer of the optimization problem (4).

**Theorem 3.1.** *Let $m \in L^2(0, L)$. Then there exists a $\gamma^* \in \mathcal{M}$ such that $\inf_{\gamma\in\mathcal{M}} J(\gamma) = J(\gamma^*)$.*

*Proof.* We have that the boundedness from below of $J$ guarantees the existence of a minimizing sequence $(\gamma_k)_{k\in\mathbb{N}}$ such that $\|\gamma_k\|_{H^1} \leq \eta\ \forall k \in \mathbb{N}$. Therefore it contains a weakly convergent subsequence which for simplicity we still denote by $(\gamma_k)_{k\in\mathbb{N}}$, such that $\gamma_k \to \gamma^*$ weakly in $H^1$. As the admissible set $\mathcal{M}$ is weakly closed, we have that $\gamma^* \in \mathcal{M}$. On the other side, from Theorem 2.1 we deduce that the sequence $(u(\gamma_k))_{k\in\mathbb{N}}$ is bounded in $L^2(0, T; H_0^2)$, and $(u_t(\gamma_k))_{k\in\mathbb{N}}$ is bounded in $L^2(0, T; H^{-2})$. This implies that there exists a subsequence of $(u(\gamma_k))_{k\in\mathbb{N}}$, which is denoted by $(u(\gamma_k))_{k\in\mathbb{N}}$, and a function $u^* \in L^2(0, T; H_0^2)$ and $u_t^* \in L^2(0, T; H^{-2})$, such that

$$u(\gamma_k) \to u^* \text{ weakly in } L^2(0, T; H_0^2), \quad u_t(\gamma_k) \to u_t^* \text{ weakly in } L^2(0, T; H^{-2}).$$

We next show that the couple $(\gamma^*, u^*)$ is a weak solution of (2). First, note that $(\gamma_k, u(\gamma_k))$ is a weak solution of (2) for all $k \in \mathbb{N}$, that is

$$\langle u_t(\gamma_k), \varphi\rangle + a(t, u(\gamma_k), \varphi) = (f(\cdot, t), \varphi) \quad \text{for all } \varphi \in H_0^2 \text{ and a.e. } t \in (0, T). \tag{28}$$

Let $\phi \in C_0^\infty(0,T)$. Multiplying identity (28) by $\phi$ and integrating over $(0,T)$, we obtain

$$\begin{aligned}\int_0^T \langle u_t(\gamma_k), \varphi\phi\rangle dt + \int_0^T\int_0^L \sigma u_{xx}(\gamma_k)\varphi_{xx}\phi dxdt + \int_0^T\int_0^L \gamma^* u_{xx}(\gamma_k)\varphi\phi dxdt \\ + \int_0^T\int_0^L (\gamma_k - \gamma^*)\, u_{xx}(\gamma_k)\varphi\phi dxdt = \int_0^T (f(\cdot,t),\varphi)\phi dt.\end{aligned} \tag{29}$$

Now, since $H^1(0,L)$ is compactly embedded in $L^2(0,L)$, $\|u(\gamma_k)\|_{L^2(0,T;H_0^2)} \leq K$ and $\varphi \in H_0^2$, we have that

$$\begin{aligned}\int_0^T\int_0^L (\gamma_k - \gamma^*)\, u_{xx}(\gamma_k)\varphi\phi dxdt &\leq \|\phi\|_{L^\infty(0,T)}\|\varphi\|_{L^\infty}\|\gamma_k - \gamma^*\|_{L^2} T^{1/2}\|u(\gamma_k)\|_{L^2(0,T;H_0^2)} \\ &\to 0 \ \text{ as } k \to \infty.\end{aligned} \tag{30}$$

Taking $k \to \infty$ in (29), we arrive at

$$\int_0^T \phi\left(\langle u_t^*, \varphi\rangle + a(t,u,\varphi) - (f(\cdot,t),\varphi)\right) dt = 0.$$

Since the last identity holds for every $\phi \in C_0^\infty(0,T)$, we deduce that

$$\langle u_t^*, \varphi\rangle + \int_0^L \sigma(x) u_{xx}\varphi_{xx} dx + \int_0^L \gamma^*(x) u_{xx}\varphi dx = (f(\cdot,t),\varphi) \ \text{ a.e. } t \in (0,T) \text{ and } \forall \varphi \in H_0^2, \tag{31}$$

and therefore $u^*(x,t) = u(x,t;\gamma^*)$. Now, we will prove that $u^*(0) = u_0$. Let $\phi \in C^1([0,T])$ such that $\phi(0) = 1$ and $\phi(T) = 0$. Then, multiplying identity (28) by $\phi$ and integrating over $(0,T)$, we get

$$\begin{aligned}&-\int_0^T\int_0^L u(\gamma_k)\varphi\phi_t dxdt + \int_0^T\int_0^L \sigma u_{xx}(\gamma_k)\varphi_{xx}\phi dxdt + \int_0^T\int_0^L \gamma^* u_{xx}(\gamma_k)\varphi\phi dxdt \\ &+ \int_0^T\int_0^L (\gamma_k - \gamma^*)\, u_{xx}(\gamma_k)\varphi\phi dxdt = \int_0^L u_0(x)\varphi dx + \int_0^T (f(\cdot,t),\varphi)\phi dt.\end{aligned}$$

Taking $k \to \infty$, then integrating by parts in time and finally using (30) and (31), we obtain

$$\int_0^L u^*(0)\varphi dx = \int_0^L u_0(x)\varphi dx \ \ \forall \varphi \in H_0^2,$$

which allows us deduce that $u^*(0) = u_0$. It remains to prove that $\gamma^*$ is optimal. Noting that $u(x,T;\gamma_k) \rightharpoonup u(x,T;\gamma^*)$ weakly in $L^2$ and the $H^1$-norm is weak lower semi-continuous, we obtain

$$\inf_{\gamma\in\mathcal{M}} J(\gamma) \leq J(\gamma^*) \leq \liminf_{k\to\infty} J(\gamma_k) = \lim_{k\to\infty} J(\gamma_k) = \inf_{\gamma\in\mathcal{M}} J(\gamma).$$

Therefore, $\gamma^*$ minimizes the functional $J$. □

## 3.2 Optimality conditions

In this subsection, we derive the first order necessary optimality conditions for the minimizer of problem (4).

Suppose that $\gamma, \gamma + \delta\gamma \in \mathcal{M}$. We observe that the variation of the functional $J$ defined by

$$\delta J(\gamma) = J(\gamma + \delta\gamma) - J(\gamma),$$

satisfies

$$\begin{aligned}\delta J(\gamma) = &\int_0^L (u(x,T;\gamma) - m(x))\delta u(x,T;\gamma)dx + \alpha(\gamma,\delta\gamma) + \alpha(\gamma',\delta\gamma') \\ &+ \frac{\alpha}{2}\|\delta\gamma\|^2_{H^1} + \frac{1}{2}\|\delta u(\cdot,T;\gamma)\|^2_{L^2},\end{aligned} \tag{32}$$

where $\delta u(x,t;\gamma) := u(x,t;\gamma+\delta\gamma) - u(x,t;\gamma)$ is solution of the following system:

$$\begin{cases} \delta u_t + (\sigma(x)\delta u_{xx})_{xx} + \gamma(x)\delta u_{xx} = -(\delta\gamma(x))u_{xx}(x,t;\gamma+\delta\gamma), & x \in (0,L)\times(0,T), \\ \delta u(0,t) = \delta u(L,t) = 0, & t \in (0,T), \\ \delta u_x(0,t) = \delta u_x(L,t) = 0, & t \in (0,T), \\ \delta u(x,0) = 0, & x \in (0,L). \end{cases} \tag{33}$$

**Remark 3.1.** *A similar well-posedness result as that obtained in Theorem 2.1 can be proved for system* (33).

**Proposition 3.1.** *The unique weak solution of* (33) *satisfies the following estimate:*

$$\|\delta u\|^2_{L^\infty(0,T;L^2)} + \|\delta u\|^2_{L^2(0,T;H^2_0)} \leq K(T,u_0,\sigma_0,f)\|\delta\gamma\|^2_{H^1}. \tag{34}$$

*Proof.* From (24) we deduce that it is sufficient to estimate the source term

$$f := -(\delta\gamma(x))u_{xx}(x,t;\gamma+\delta\gamma).$$

In fact

$$\begin{aligned}\|\delta\gamma(\cdot)u_{xx}(\cdot,\cdot;\gamma+\delta\gamma)\|^2_{L^2(0,T;L^2)} &= \int_0^T\int_0^L |(\delta\gamma(x))u_{xx}(x,t;\gamma+\delta\gamma)|^2 dxdt \\ &\leq \|\delta\gamma\|^2_{L^\infty}\int_0^T\int_0^L |u_{xx}(x,t;\gamma+\delta\gamma)|^2 dxdt \\ &\leq K(T,u_0,\sigma_0,f)\|\delta\gamma\|^2_{H^1}.\end{aligned}$$

The last line follows from Theorem 2.1 and the continuous embedding of $H^1(0,L)$ in $L^\infty(0,L)$. □

In order to obtain the derivative of the functional $J$ and deduce the optimality conditions for the minimizer of problem (4), we introduce an adjoint system. Let $\phi_T \in L^2$. Let $\phi = \phi(x,t;\gamma)$ the unique weak solution of the following system:

$$\begin{cases} -\phi_t + (\sigma(x)\phi_{xx})_{xx} + (\gamma(x)\phi)_{xx} = 0, & (x,t) \in (0,L)\times(0,T), \\ \phi(0,t) = \phi(L,t) = 0, & t \in (0,T), \\ \phi_x(0,t) = \phi_x(L,t) = 0, & t \in (0,T), \\ \phi(x,T) = \phi_T(x), & x \in (0,L). \end{cases} \tag{35}$$

In a similar way as done for system (2), the following energy estimate can be shown for the adjoint system (35) (see Theorem 2.1):

**Proposition 3.2.** *Let $\phi_T \in L^2(0,L)$. Then, the unique weak solution $\phi$ of* (35) *satisfies the following estimate:*

$$\|\phi_t\|^2_{L^2(0,T;H^{-2})} + \|\phi\|^2_{L^\infty(0,T;L^2)} + \|\phi\|^2_{L^2(0,T;H^2_0)} \leq K(T,\eta,\sigma_0)\|\phi_T\|^2_{L^2}. \tag{36}$$

The following proposition determines an integral relationship between (2) and the adjoint system (35).

**Proposition 3.3.** *Let $u_0, \phi_T \in L^2(0,L)$. Let $\delta u$ be solution of (33) and $\phi$ be a solution of (35). Then, the following identity hold:*

$$\begin{aligned}\int_0^L \phi_T(x)\delta u(x,T;\gamma)dx &= -\int_0^T\int_0^L u_{xx}(x,t;\gamma+\delta\gamma)\phi(x,t)\delta\gamma(x)dxdt \\ &= -\int_0^T\int_0^L u_{xx}(x,t;\gamma)\phi(x,t)\delta\gamma(x)dxdt \\ &\quad -\int_0^T\int_0^L \delta u_{xx}(x,t;\gamma)\phi(x,t)\delta\gamma(x)dxdt.\end{aligned} \tag{37}$$

*Moreover, there exists a constant $K$ such that*

$$\left|\int_0^T\int_0^L \delta u_{xx}(x,t;\gamma)\phi(x,t)\delta\gamma(x)dxdt\right| \leq K(T,\eta,u_0,\sigma_0)\|\phi_T\|_{L^2}\|\delta\gamma\|^2_{H^1}. \tag{38}$$

*Proof.* Multiplying equation (33) by $\phi$ and integrating over $(0,L)\times(0,T)$, we obtain

$$\int_0^T\int_0^L \left(\delta u_t + (\sigma\delta u_{xx})_{xx} + \gamma(x)\delta u_{xx}\right)\phi dxdt = -\int_0^T\int_0^L u_{xx}(x,t;\gamma+\delta\gamma)\phi\delta\gamma(x)dxdt. \tag{39}$$

After some integration by parts in time on the left-hand side of (39), we get

$$\begin{aligned}\int_0^T\int_0^L \left(\delta u_t + (\sigma\delta u_{xx})_{xx} + \gamma(x)\delta u_{xx}\right)\phi dxdt &= \int_0^T\int_0^L \left(-\phi_t + (\sigma\phi_{xx})_{xx} + (\gamma(x)\phi)_{xx}\right)\delta u dxdt \\ &\quad + \int_0^L \phi_T(x)\delta u(x,T;\gamma)dx + \int_0^T \gamma(x)\delta u_x\phi\Big|_{x=0}^{x=L} \\ &= \int_0^L \phi_T(x)\delta u(x,T;\gamma)dx.\end{aligned} \tag{40}$$

Combining (39) with (40), we obtain the identity (37). Now, we will prove (38). From (34) and (36), we deduce the following estimate:

$$\begin{aligned}\int_0^T\int_0^L \delta u_{xx}(x,t;\gamma)\phi(x,t)\delta\gamma(x)dxdt &\leq \|\delta\gamma\|_{L^\infty}\int_0^T\int_0^L |\delta u_{xx}(x,t)\phi(x,t)|\,dxdt \\ &\leq \|\delta\gamma\|_{L^\infty}\int_0^T \|\delta u_{xx}(\cdot,t)\|_{L^2}\|\phi(\cdot,t)\|_{L^2}dt \\ &\leq \|\delta\gamma\|_{L^\infty}\max_{0\leq t\leq T}\|\phi(t)\|_{L^2}\sqrt{T}\|\delta u\|_{L^2(0,T;H_0^2)} \\ &\leq \sqrt{T}\|\delta\gamma\|_{L^\infty}K_1(T,\eta,\sigma_0)\|\phi_T\|_{L^2}K_2(T,\eta,u_0)\|\delta\gamma\|_{L^\infty} \\ &\leq K_3(T,\eta,u_0,\sigma_0)\sqrt{T}\|\phi_T\|_{L^2}\|\delta\gamma\|^2_{L^\infty}.\end{aligned}$$

Finally, since the embedding $H^1(0,L)$ in $L^\infty(0,L)$ is continuous, we conclude (38). □

**Proposition 3.4.** *Let $u_0 \in L^2(0,L)$. Then the variation of functional $J$ satisfies the following:*

$$\delta J(\gamma) = \left(-\int_0^T u_{xx}(x,t;\gamma)\phi(x,t)dt, \delta\gamma(\cdot)\right) + \alpha\left(\gamma,\delta\gamma\right) + \alpha\left(\gamma',\delta\gamma'\right) + o\left(\|\delta\gamma\|_{H^1}\right), \tag{41}$$

*where $\phi$ is the solution of the adjoint problem (35) with final data $\phi_T(\cdot) = u(\cdot,T;\gamma) - m(\cdot)$ in $(0,L)$. Moreover, the Fréchet derivative of the functional $J$ in $\gamma \in \mathcal{M}$ is given by*

$$J'(\gamma)\delta\gamma = -\int_0^T\int_0^L u_{xx}(x,t;\gamma)\phi(x,t)\delta\gamma(x)dxdt + \alpha\left(\gamma,\delta\gamma\right) + \alpha\left(\gamma',\delta\gamma'\right), \tag{42}$$

*for all* $\delta\gamma \in \mathcal{M}$.

*Proof.* Taking $\phi_T(\cdot) = u(\cdot, T; \gamma) - m(\cdot)$ in $(0, L)$ and using (37) in (32), we obtain that the variation $\delta J(\gamma)$ can be written as

$$\delta J(\gamma) = -\int_0^T \int_0^L u_{xx}(x,t;\gamma)\phi(x,t)\delta\gamma(x)dxdt + \alpha\left(\gamma, \delta\gamma\right) + \alpha\left(\gamma', \delta\gamma'\right) + R(\delta\gamma),$$

where

$$R(\delta\gamma) = \frac{1}{2}\|\delta u(\cdot, T; \gamma)\|_{L^2}^2 - \int_0^T \int_0^L \delta u_{xx}(x,t;\gamma)\phi(x,t)\delta\gamma(x)dxdt + \frac{\alpha}{2}\|\delta\gamma\|_{H^1}^2.$$

Using (34) and (38), we get

$$\begin{aligned} |R(\delta\gamma)| &\leq \frac{1}{2}\|\delta u(x, T; \gamma)\|_{L^2}^2 + \left|\int_0^T \int_0^L \delta u_{xx}(x,t;\gamma)\phi(x,t)\delta\gamma(x)dxdt\right| + \frac{\alpha}{2}\|\delta\gamma\|_{H^1}^2 \\ &\leq \left(\frac{1}{2}K_1(T, \eta, u_0, \sigma_0) + K_2(T, \eta, u_0, \sigma_0)\|\phi_T\|_{L^2} + \frac{\alpha}{2}\right)\|\delta\gamma\|_{H^1}^2. \end{aligned}$$

Using estimate (24), we obtain

$$\|\phi_T\|_{L^2}^2 \leq 2\left(\|u(\cdot, T; \gamma)\|_{L^2}^2 + \|m\|_{L^2}^2\right) \leq K_3(T, \eta, u_0, \sigma_0).$$

From this last estimate, we obtain

$$|R(\delta\gamma)| \leq K_4(T, \eta, u_0, \alpha, \sigma_0)\|\delta\gamma\|_{H^1}^2.$$

This completes the proof of (42). □

We are now ready to state the first order necessary optimality conditions for the minimizer of (4).

**Proposition 3.5.** *Let* $\gamma$ *solution of the optimization problem* (4) *and* $u = u(\gamma)$ *the corresponding solution of* (2). *Then, we have*

$$-\int_0^T \int_0^L u_{xx}(x,t;\gamma)\phi(x,t)(h-\gamma)(x)dxdt + \alpha\left(\gamma, h-\gamma\right) + \alpha\left(\gamma', h'-\gamma'\right) \geq 0, \tag{43}$$

*for all* $h \in \mathcal{M}$, *where* $\phi$ *is the solution of the adjoint system* (35) *with* $\phi_T(x) = u(x, T; \gamma) - m(x)$, $x \in (0, L)$.

*Proof.* Let $\gamma$ be a solution of the optimization problem (4) and $u = u(\gamma)$ the corresponding solution of (2). Let $\gamma_\lambda = \gamma + \lambda(h-\gamma)$ with $\lambda \in [0, 1]$ and $h \in \mathcal{M}$. We consider $u_\lambda = u(x, t; \gamma_\lambda)$. Since $J$ is Fréchet differentiable in $\gamma_\lambda$ we have

$$\frac{d}{d\lambda}J(\gamma_\lambda)\Big|_{\lambda=0} = \frac{1}{2}\int_0^L (u_\lambda(x,T) - m(x))\frac{\partial u_\lambda}{\partial\lambda}\Big|_{\lambda=0}dx + \alpha\left(\gamma, h-\gamma\right) + \alpha\left(\gamma', h'-\gamma'\right). \tag{44}$$

If we set $\widetilde{u_\lambda} = \frac{\partial u_\lambda}{\partial\lambda}$, then this function solves

$$\begin{cases} (\widetilde{u}_\lambda)_t + (\sigma(\widetilde{u}_\lambda)_{xx})_{xx} + (h-\gamma)(u_\lambda)_{xx} + (\gamma + \lambda(h-\gamma))(\widetilde{u}_\lambda)_{xx} = 0, & (x,t) \in (0,L)\times(0,T), \\ \widetilde{u}_\lambda(0,t) = \widetilde{u}_\lambda(L,t) = 0, & t \in (0,T), \\ (\widetilde{u}_\lambda)_x(0,t) = (\widetilde{u}_\lambda)_x(L,t) = 0, & t \in (0,T), \\ \widetilde{u}_\lambda(x,0) = 0, & x \in (0,L). \end{cases}$$

Now, if we define $\rho = \widetilde{u_\lambda}|_{\lambda=0}$ we see that

$$\begin{cases} \rho_t + (\sigma\rho_{xx})_{xx} + \gamma(x)\rho_{xx} = -(h-\gamma)u_{xx}, & (x,t) \in (0,L)\times(0,T), \\ \rho(0,t) = \rho(L,t) = 0, & t \in (0,T), \\ \rho_x(0,t) = \rho_x(L,t) = 0, & t \in (0,T), \\ \rho(x,0) = 0, & x \in (0,L). \end{cases} \tag{45}$$

Since $\gamma$ is optimal we have that

$$\frac{d}{d\lambda} J(\gamma_\lambda)\Big|_{\lambda=0} \geq 0, \quad \forall h \in \mathcal{M},$$

i.e.,

$$\int_0^L (u(x,T;\gamma) - m(x))\rho(x,T)dx + \alpha\,(\gamma, h-\gamma) + \alpha\,(\gamma', h'-\gamma') \geq 0.$$

Using the adjoint system (35) with the final condition $\phi(x,T) = u(x,T;\gamma) - m(x)$, $x \in (0,L)$, we have

$$\int_0^L \phi(x,T)\rho(x,T)dx + \alpha\,(\gamma, h-\gamma) + \alpha\,(\gamma', h'-\gamma') \geq 0, \quad \forall h \in \mathcal{M}. \tag{46}$$

Multiplying the first equation in (35) by $\rho$ and integrating by parts over $(0,L)\times(0,T)$, we get

$$\int_0^L \phi(x,T)\rho(x,T)dx = -\int_0^T \int_0^L u_{xx}(x,t;\gamma)\phi(x,t)(h(x)-\gamma(x))dxdt. \tag{47}$$

Finally, the result it follows from (46) and (47). □

### 3.3 Local stability result

In this subsection, we prove the stability result stated in Theorem 1.1.

Let $u$ and $\widetilde{u}$ be the solutions of the system (2) corresponding to the coefficients $\gamma$ and $\widetilde{\gamma}$, respectively. Given the measurements $m$ and $\widetilde{m}$, we define by $\phi$ and $\widetilde{\phi}$ the corresponding solutions of the adjoint system (35) with final data

$$\phi_T(\cdot) = u(\cdot,T;\gamma) - m(\cdot) \quad \text{and} \quad \widetilde{\phi_T}(\cdot) = \widetilde{u}(\cdot,T;\widetilde{\gamma}) - \widetilde{m}(\cdot), \ \text{ in } (0,L),$$

respectively. Let $U = u - \widetilde{u}$, $Q = \gamma - \widetilde{\gamma}$ and $V = \phi - \widetilde{\phi}$. We note that $U$ and $V$ satisfies respectively the following equations:

$$\begin{cases} U_t + (\sigma(x)U_{xx})_{xx} + \gamma(x)U_{xx} = -Q\widetilde{u}_{xx}, & (x,t) \in (0,L)\times(0,T), \\ U(0,t) = U(L,t) = 0, & t \in (0,T), \\ U_x(0,t) = U_x(L,t) = 0, & t \in (0,T), \\ U(x,0) = 0, & x \in (0,L), \end{cases} \tag{48}$$

and

$$\begin{cases} -V_t + (\sigma(x)V_{xx})_{xx} + (\gamma(x)V)_{xx} = -\left(Q\widetilde{\phi}\right)_{xx}, & (x,t) \in (0,L)\times(0,T), \\ V(0,t) = V(L,t) = 0, & t \in (0,T), \\ V_x(0,t) = V_x(L,t) = 0, & t \in (0,T), \\ V(x,T) = U(x,T) - (m(x) - \widetilde{m}(x)), & x \in (0,L). \end{cases} \tag{49}$$

In the following propositions we obtain some energy type estimates for the systems (48) and (49).

**Proposition 3.6.** *Let $\gamma, \widetilde{\gamma} \in L^\infty(0,L)$. Then, there exists a positive constant $K_1$ independent of $T$, such that the solution of (48) satisifies*

$$\|U(t)\|_{L^2}^2 + \int_0^T \int_0^L |U_{xx}|^2 dxdt \leq \left( e^{K_1 T} + \frac{K_1 T}{\sigma_0} + \frac{1}{\sigma_0} \right) \|Q\|_{L^\infty}^2 \|\widetilde{u}\|_{L^2(0,T;H_0^2)}^2. \tag{50}$$

*Proof.* Multiplying the first equation in (48) by $U$ and integrating by parts over $(0,L)$ we get

$$\frac{1}{2}\frac{d}{dt}\int_0^L |U|^2 dx + \int_0^L \sigma(x)|U_{xx}|^2 dx = -\int_0^L \gamma(x) U_{xx} U dx - \int_0^L Q(x)\widetilde{u}_{xx} U dx.$$

If we consider the following estimate on the right side of the last identity

$$\begin{aligned} -\int_0^L \gamma(x) U_{xx} U dx - \int_0^L Q\widetilde{u}_{xx} U dx \leq \frac{\|\gamma\|_{L^\infty}^2}{2\sigma_0} \int_0^L |U|^2 dx + \frac{1}{2}\int_0^L \sigma |U_{xx}|^2 dx \\ + \frac{1}{2}\int_0^L |U|^2 dx + \frac{\|Q\|_{L^\infty}^2}{2} \int_0^L |\widetilde{u}_{xx}|^2 dx, \end{aligned}$$

then we obtain

$$\frac{d}{dt}\int_0^L |U|^2 dx + \int_0^L \sigma(x)|U_{xx}|^2 dx \leq \left[ \frac{\|\gamma\|_{L^\infty}^2}{\sigma_0} + 1 \right] \int_0^L |U|^2 dx + \|Q\|_{L^\infty}^2 \int_0^L |\widetilde{u}_{xx}|^2 dx. \tag{51}$$

Using the Gronwal's inequality in (51), we get

$$\int_0^L |U|^2 dx \leq \exp(K_1 T) \|Q\|_{L^\infty}^2 \int_0^T \int_0^L |\widetilde{u}_{xx}|^2 dxdt, \tag{52}$$

where

$$K_1 = \frac{\|\gamma\|_{L^\infty}^2}{\sigma_0} + 1.$$

Integrating over $(0,T)$ in (52), we obtain

$$\int_0^T \int_0^L |U_{xx}|^2 dxdt \leq \frac{K_1 T}{\sigma_0} e^{K_1 T} \|Q\|_{L^\infty}^2 \|\widetilde{u}\|_{L^2(0,T;H_0^2)}^2 + \frac{1}{\sigma_0} \|Q\|_{L^\infty}^2 \|\widetilde{u}\|_{L^2(0,T;H_0^2)}^2. \tag{53}$$

Finally, combining (52) and (53) we deduce (50). □

**Proposition 3.7.** *Let $\gamma, \widetilde{\gamma} \in L^\infty(0,L)$ and $m, \widetilde{m} \in L^2(0,L)$. Then, there exists positive constants $K_1$ and $K_2$ independents of $T$, such that the solution $V$ of (49) satisfies*

$$\begin{aligned} \|V(t)\|_{L^2}^2 \leq 2e^{K_2 T} \left( e^{K_1 T} + \frac{K_1 T}{\sigma_0} + \frac{1}{\sigma_0} \right) \|\widetilde{u}\|_{L^2(0,T;H_0^2)}^2 \|Q\|_{L^\infty}^2 \\ + \frac{2T}{\sigma_0} \|Q\|_{L^\infty}^2 \|\widetilde{\phi}\|_{L^\infty(0,T;L^2)}^2 + 2e^{K_2 T} \|m - \widetilde{m}\|_{L^2}^2. \end{aligned} \tag{54}$$

*Proof.* If we consider the change of variable $t \mapsto T - t$ we see that $V := V(x, T-t)$ solves the system (49) with initial condition given by $V(x,0) = U(x,T) - (m(x) - \widetilde{m}(x))$. Multiplying the first equation in (49) by $V$ and integrating by parts over $(0,L)$, we get

$$\frac{1}{2}\frac{d}{dt}\int_0^L |V|^2 dx + \int_0^L \sigma(x)|V_{xx}|^2 dx = -\int_0^L \gamma(x) V V_{xx} dx - \int_0^L Q\widetilde{\phi} V_{xx} dx. \tag{55}$$

If we consider in the last inequality that

$$-\int_0^L \gamma(x)VV_{xx}dx - \int_0^L Q\widetilde{\phi}V_{xx}dx \leq \frac{\|\gamma\|_{L^\infty}^2}{\sigma_0}\int_0^L |V|^2dx + \frac{1}{4}\int_0^L \sigma(x)|V_{xx}|^2dx + \frac{\|Q\|_{L^\infty}^2}{\sigma_0}\int_0^L |\widetilde{\phi}|^2dx + \frac{1}{4}\int_0^L \sigma(x)|V_{xx}|^2dx,$$

then we arrive to

$$\frac{d}{dt}\int_0^L |V|^2dx + \int_0^L \sigma(x)|V_{xx}|^2dx \leq \frac{2\|\gamma\|_{L^\infty}^2}{\sigma_0}\int_0^L |V|^2dx + \frac{2\|Q\|_{L^\infty}^2}{\sigma_0}\int_0^L |\widetilde{\phi}|^2dx. \tag{56}$$

Using the Gronwall's inequality for estimate the first term on the right side in (56) we obtain

$$\int_0^L |V|^2dx \leq \exp\left[\frac{2T\|\gamma\|_{L^\infty}^2}{\sigma_0}\right]\int_0^L |U(x,T) - (m(x) - \widetilde{m}(x))|^2\,dx + \frac{2\|Q\|_{L^\infty}^2}{\sigma_0}\int_0^T\int_0^L |\widetilde{\phi}|^2dxdt. \tag{57}$$

Finally, using Proposition 3.6, we estimate the right side in (57) and we get (54). □

Now, we present the proof of Theorem 1.1.

**Proof Theorem 1.1**. Let $u$ and $\widetilde{u}$ be the solutions of (2) corresponding to the coefficients $\gamma$ and $\widetilde{\gamma}$, respectively. Let $\phi$ and $\widetilde{\phi}$ be the solutions of the corresponding auxliar system (35). Since $\gamma$ and $\widetilde{\gamma}$ satisfies the optimality condition (44) we have that

$$-\int_0^T\int_0^L u_{xx}\phi(\widetilde{\gamma} - \gamma)dxdt + \alpha\int_0^L \gamma'(\widetilde{\gamma}' - \gamma')dx + \alpha\int_0^L \gamma(\widetilde{\gamma} - \gamma)dx \geq 0 \tag{58}$$

and

$$-\int_0^T\int_0^L \widetilde{u}_{xx}\widetilde{\phi}(\gamma - \widetilde{\gamma})dxdt + \alpha\int_0^L \widetilde{\gamma}'(\gamma' - \widetilde{\gamma}')dx + \alpha\int_0^L \widetilde{\gamma}(\gamma - \widetilde{\gamma})dx \geq 0. \tag{59}$$

Combining (58) and (59), we get

$$\alpha\|\gamma - \widetilde{\gamma}\|_{H^1}^2 \leq \int_0^T\int_0^L (U_{xx}\phi Q + \widetilde{u}_{xx}VQ)dxdt. \tag{60}$$

Using the Höder's inequality, (24), (36) and Proposition 3.6, we have

$$\begin{aligned}\int_0^T\int_0^L U_{xx}\phi Q dxdt &\leq \frac{1}{2\sqrt{T}}\int_0^T\int_0^L |U_{xx}|^2dxdt + \sqrt{T}\frac{\|Q\|_{L^\infty}^2}{2}\int_0^T\int_0^L |\phi|^2dxdt \\ &\leq \frac{1}{2\sqrt{T}}\left(e^{K_1T} + \frac{K_1T}{\sigma_0} + \frac{1}{\sigma_0}\right)\|Q\|_{L^\infty}^2\|\widetilde{u}\|_{L^2(0,T;H_0^2)}^2 \\ &+ T\sqrt{T}\frac{\|Q\|_{L^\infty}^2}{2}\left(1 + \frac{TK_2}{\sigma_0}\right)e^{K_2T}\|u(\cdot,T) - m(\cdot)\|_{L^2}^2 \\ &\leq K_3\sqrt{T}e^{K_4T}\left(e^{K_1T} + \frac{K_1T}{\sigma_0} + \frac{1}{\sigma_0}\right)\|Q\|_{L^\infty}^2 \\ &+ K_5T^2\sqrt{T}e^{K_6T}\left(1 + \frac{TK_2}{\sigma_0}\right)\|Q\|_{L^\infty}^2.\end{aligned} \tag{61}$$

Similarly, using inequality (54) instead (50), we have

$$\begin{aligned}\int_0^T\int_0^L \widetilde{u}VQdxdt &\leq \frac{1}{2}\int_0^T\int_0^L |V|^2dxdt + \frac{\|Q\|_{L^\infty}^2}{2}\int_0^T\int_0^L |\widetilde{u}_{xx}|^2dxdt\\ &\leq C_1T\left(e^{C_2T}+T\right)\|\widetilde{u}\|^2_{L^2(0,T;H_0^2)}\|Q\|^2_{L^\infty} + C_3\|Q\|^2_{L^\infty}\|\widetilde{\phi}\|^2_{L^\infty(0,T;L^2)}\\ &+ C_4e^{C_5T}\|m-\widetilde{m}\|^2_{L^2}\\ &\leq C_6Te^{C_7T}\left(e^{C_2T}+T\right)\|Q\|^2_{L^\infty} + C_8Te^{C_9T}\|Q\|^2_{L^\infty} + C_4e^{C_5T}\|m-\widetilde{m}\|^2_{L^2}.\end{aligned} \tag{62}$$

Then, by using (61) and (62) for estimating the right side on (60), and the continuous injection of $H^1(0,L)$ in $L^\infty(0,L)$ we obtain

$$\|\gamma-\widetilde{\gamma}\|^2_{H^1} \leq \frac{K_T}{\alpha}\|Q\|^2_{H^1} + \frac{Ce^{CT}}{\alpha}\|m-\widetilde{m}\|^2_{L^2}, \tag{63}$$

where

$$\begin{aligned}K_T = K_3\sqrt{T}e^{K_4T}\left(e^{K_1T}+\frac{K_1T}{\sigma_0}+\frac{1}{\sigma_0}\right) + K_5T^2\sqrt{T}e^{K_6T}\left(1+\frac{TK_2}{\sigma_0}\right)\\ + C_6Te^{C_7T}\left(e^{C_2T}+T\right) + C_8Te^{C_9T}.\end{aligned}$$

Finally, choosing $T=T_0>0$ such that $\dfrac{K_T}{\alpha}<1$ in (63), we conclude the proof.

# 4 Numerical algorithm and simulations

In this section we introduce a numerical scheme to recover the anti-diffusion coefficient $\gamma=\gamma(x)$ in the linear Kuramoto-Sivashinsky equation (2) with $f\equiv 0$. First, we need to introduce the variational formulation for solving the forward problem (2) for a given coefficient $\gamma$. In order to decrease the order of differentiation in the Kuramoto-Sivashinsky equation, it is convenient to rewrite it as a system of two coupled second-order partial differential equations by introducing the variable $v:=u_{xx}$. Thus, we obtain the system

$$\begin{cases} v = u_{xx}, & (x,t)\in(0,L)\times(0,T),\\ u_t+(\sigma(x)v)_{xx}+\gamma(x)v=0, & (x,t)\in(0,L)\times(0,T).\end{cases} \tag{64}$$

By multiplying the first and second equation in (64) by functions $w\in H^1$ and $\varphi\in H_0^1$, respectively, and then integrating by parts on the interval $(0,L)$, we obtain

$$\begin{cases} \displaystyle\int_0^L vwdx + \int_0^L u_xw_xdx = 0, & \text{a.e. } t\in(0,T),\\ \displaystyle\int_0^L u_t\varphi dx - \int_0^L(\sigma(x)v)_x\varphi_xdx + \int_0^L\gamma(x)v\varphi dx = 0, & \text{a.e. } t\in(0,T).\end{cases} \tag{65}$$

By following Rothe's strategy [22] (also called horizontal line method, or the method of semidiscretization), we first discretize the temporal variable in the previous system with the second-order two-step implicit method of leap-frog type

$$\begin{cases} \displaystyle\int_0^L\Big(\frac{v^{n+1}+v^{n-1}}{2}\Big)w + \int_0^L u_x^{n+1}w_xdx = 0,\\ \displaystyle\int_0^L\Big(\frac{u^{n+1}-u^{n-1}}{2\Delta t}\Big)\varphi dx - \frac{1}{2}\int_0^L\Big(\sigma(x)(v^{n+1}+v^{n-1})\Big)_x\varphi_xdx\\ \displaystyle+\int_0^L\gamma(x)\Big(\frac{v^{n+1}+v^{n-1}}{2}\Big)\varphi dx = 0,\end{cases} \tag{66}$$

given that $u^0 = u_0(x), v^0 = u_{0,xx}(x)$. Here $u^n$ denotes the approximation of $u(x,t)$ at time $t = n\Delta t$. To compute the values $u^1, v^1$ necessary for starting the two-step method (66), we use the implicit second-order one-step method

$$\begin{cases} \displaystyle\int_0^L \Big(\frac{v^{n+1}+v^n}{2}\Big)w + \int_0^L u_x^{n+1} w_x dx = 0, \\ \displaystyle\int_0^L \Big(\frac{u^{n+1}-u^n}{\Delta t}\Big)\varphi dx - \frac{1}{2}\int_0^L \Big(\sigma(x)(v^{n+1}+v^n)\Big)_x \varphi_x dx \\ \displaystyle + \int_0^L \gamma(x)\Big(\frac{v^{n+1}+v^n}{2}\Big)\varphi dx = 0. \end{cases} \tag{67}$$

To discretize the spatial variable in the variational formulation (67), we use the Finite Element Method (FEM) as implemented by the Python-FeniCS-DOLFIN system [2], [18] which uses Rothe's approach. The FEniCS project is a collection of software tools for automating the solution of differential equations [17]. These components include the Unified Form Language (UFL) [1], [3], the FEniCS compiler (FFC) [14] and DOLFIN [19], [20]. In the FEM for problem (2), the interval $[0, L]$ is discretized by an equally-spaced partition $x_j$, $j = 1, ..., N$, and the solution component $u(x,t)$ at time $t = n\Delta t$ is approximated by

$$u^n(x) = \sum_{j=1}^{N} u_j^n S_j(x), \tag{68}$$

where $S_j(x)$ is the system of first-order piecewise linear Lagrange polynomials given by

$$S_j(x) = \begin{cases} \dfrac{x - x_{j-1}}{x_j - x_{j-1}}, & x \in [x_{j-1}, x_j], \\ \dfrac{x - x_{j+1}}{x_j - x_{j+1}}, & x \in [x_j, x_{j+1}], \\ 0, & \text{in other case,} \end{cases}$$

and the second component $v = v(x,t)$ can be similarly approximated. It is important to point out that the temporal discretization (66) for the system formulation of the KS equation given in (64) has better numerical stability properties than the same approach applied directly to the scalar KS equation.

In order to illustrate the process of approximating numerically the solution of the inverse problem studied for the KS equation by using an optimization-based approach, we will conduct some numerical experiments by considering a regularized Tikhonov-type functional in the form

$$\mathcal{J}_1(\gamma) := \frac{1}{2}\|u(\cdot, T; \gamma) - m\|_{L^2}^2 + \frac{\alpha}{2}\|\gamma - \gamma_0\|_{L^2}^2 + \frac{\alpha}{2}\|\gamma'\|_{L^2}^2, \tag{69}$$

which is minimized constrained by the KS equation. Here, $\gamma_0 \in L^2$ is the initial guess employed for starting the minimization process of the functional $\mathcal{J}_1$ and $\alpha > 0$.

Observe that the functional $\mathcal{J}_1$ is analogous to the functional (3) already analyzed in the previous sections from the analytical point of view. We point out that the stability result given in Theorem 1.1 is also valid for the case of the functional $\mathcal{J}_1$, provided that $\gamma_0 \in L^2$.

In some of the numerical experiments for obtaining a more accurate identification of the coefficient $\gamma$, we need to use instead the following regularized functionals

$$\mathcal{J}_2(\gamma) := \frac{1}{2}\|u(\cdot, T; \gamma) - m\|_{L^2}^2 + \frac{\alpha}{2}\|\gamma - \gamma_0\|_{L^2}^2, \tag{70}$$

$$\mathcal{J}_3(\gamma) := \frac{1}{2}\|u(\cdot, T; \gamma) - m\|_{H^1}^2 + \frac{\alpha}{2}\int_0^L \sqrt{(\gamma(x) - \gamma_0)^2 + \epsilon}\, dx, \tag{71}$$

and

$$\mathcal{J}_4(\gamma) := \frac{1}{2}\|u(\cdot,T;\gamma) - m\|_{L^2}^2 + \frac{\alpha}{2}\int_0^L \sqrt{(\gamma(x)-\gamma_0)^2+\epsilon}\, dx, \tag{72}$$

where $\epsilon > 0$. Although functionals $\mathcal{J}_2$, $\mathcal{J}_3$, $\mathcal{J}_4$ do not satisfy the hypothesis of Theorem 1.1, we include the corresponding experiments since they result to be appropriate for parameter identification. It would be an interesting problem to search for a stability result analogous to Theorem 1.1 for these cases. We recall also that the functional $\mathcal{J}_3$ is employed only in experiment 2, where the observation $m$ is differentiable. In other numerical simulations we used functionals $\mathcal{J}_1$, $\mathcal{J}_2$ and $\mathcal{J}_4$ where the mismatch between the final time and observation is measured by using the $L^2$-norm.

The minimization of the above functionals is performed with the help of the Dolfin-Adjoint library (see [9], [10] ) and the iterative L-BFGS-B algorithm from the SciPy (Scientific Computing Tools for Python) library [25], described by Byrd et al. [5], and Zhu et al. [27]. We choose to work with the L-BFGS-B algorithm mainly because we do not need to provide information about the Hessian and the structure of our objective funcional. Also, storage requirements are low and in general this scheme outperforms other Hessian-free Newton methods for large scale problems. The Dolfin-Adjoint project automatically derives the discrete adjoint and tangent linear models written in the Python interface to DOLFIN. We point out that this kind of approach has already been applied successfully in [21] to identity the linear velocity coefficient in a scalar dispersive linear Benjamin-Bona-Mahony equation.

In all numerical experiments, we set the length of the spatial domain $L = 3.0$, the initial condition $u(x,0) = e^{-30(x-1)^2}$, $x \in (0,L)$, and the initial guess for the unknown coefficient $\gamma$ in the minimization process of the objective functional is taken as $\gamma_0 \equiv 1$. All relative errors are computed in the supremum norm. In order to illustrate the efficiency of the numerical strategy proposed, we compute an approximation of the solution $u(\cdot,t;\gamma)$ of the forward problem (2) within the time interval $[0,T]$, corresponding to a given coefficient $\gamma$ by using the numerical scheme given in (66). The resulting profile $m(\cdot) = u(\cdot,T;\gamma)$ in $(0,L)$ at time $t = T$ is taken as our final time measurement (target profile) for the numerical identification process of the anti-diffusion coefficient $\gamma$.

**Experiment set 1:** (Gaussian coefficient) In this experiment we set $T = 1.5$, $\sigma = 0.5$ and we take $N = 300$ equally spaced points for spatial discretization of the KS equation on the interval $[0,3]$. The exact anti-diffusion coefficient $\gamma$ is given by the Gaussian profile

$$\gamma(x) = 1 + 2e^{-5(x-1.5)^2},$$

and the time step is $\Delta t = 1.5/800 = 1.875 \times 10^{-3}$ in the numerical solution $u(\cdot,t;\gamma)$ along the time interval $[0,T]$ of both the forward and adjoint problems for the KS equation (2) with the scheme given in (66). In Figure 1(a) is displayed the result of the minimization after 60 iterations of the L-BFGS-B algorithm for the objective functional $\mathcal{J}_1$ restricted to the KS equation, and regularization parameter $\alpha = 10^{-9}$. See that the relative error between the expected and the computed coefficient $\gamma$ is approximately $3.62 \times 10^{-2}$, and thus we have a good accuracy in the identification process. In Figure 1(b), we compare the final measurement (target profile) $m$ with the corresponding solution $u(\cdot,t;\gamma)$ computed at time $t = T = 1.5$, for the coefficient $\gamma$ displayed with pointed line in Figure 1(a). We found that the relative error between these two profiles is about $3.5 \times 10^{-5}$.

**Experiment set 2:** (A chain of Gaussian profiles) In this experiment we set $T = 0.4$, $\sigma = 0.4$ and the numerical parameters are $N = 200$ and $\Delta t = 0.4/2000 = 2 \times 10^{-4}$. In this

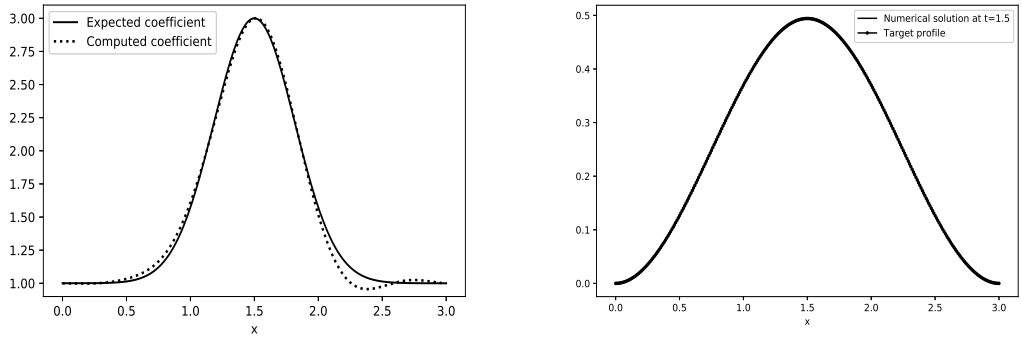


(a) (b)

Figure 1: Experiment 1 : (a) Coefficient $\gamma$ (pointed line) computed after 60 iterations of the L-BFGS-B scheme, compared with the expected coefficient (solid line). (b) Final time measurement $m$ (target profile) compared with the numerical solution $u(\cdot, T; \gamma)$ of problem (2) at the final time $T = 1.5$.

case, the exact coefficient is given by

$$\gamma(x) = 1 + e^{-10(x-1.5)^2} + 0.5e^{-30(x-0.5)^2} + 0.7e^{-40(x-2.5)^2},$$

and we perform the identification process of the coefficient $\gamma$ by computing a minimum of the functional $\mathcal{J}_3$ with regularization parameters $\alpha = 10^{-8}$ and $\epsilon = 10^{-5}$. The coefficient computed after 70 iterations of the L-BFGS-B method is shown in Figure 2. In (a) the relative error between the exact and computed coefficient is about $6 \times 10^{-2}$, and the relative error between the profiles in (b) is roughly $9 \times 10^{-7}$. Thus, again the coefficient $\gamma$ is recovered with good accuracy. In this case where the observation $m$ is smooth, we found that the functional $\mathcal{J}_4$ gave better adjustment between the exact and computed coefficients than with the rest of functionals.

**Experiment set 3:** (A non-differentiable coefficient) We now consider the identification of a coefficient in the form

$$\gamma(x) = \begin{cases} 1, & 0 \leq x < 1, \\ 2x - 1, & 1 \leq x < 1.5 \\ 5 - 2x, & 1.5 \leq x < 2, \\ 1, & 2 \leq x \leq 3, \end{cases} \tag{73}$$

which is non-differentiable. The final time is $T = 1.5$, the diffusion parameter is $\sigma = 0.3$ and the parameters for the numerical solution of the forward and adjoint problems are $N = 600$ and $\Delta t = 1.5/800 = 1.875 \times 10^{-3}$. In this case, we use $\mathcal{J}_4$ with $\alpha = 10^{-9}$, $\epsilon = 10^{-5}$ as the regularized Tikhonov functional for the identification process of the coefficient $\gamma$. The result after 70 iterations of the L-BFGS-B algorithm of the minimization procedure of this functional is displayed in Figure 3. The relative error in (a) is $5.12 \times 10^{-2}$ and in (b) the relative error is $1.2 \times 10^{-5}$, which also shows that in this case, the coefficient $\gamma$ is also recovered with good accuracy.

**Experiment set 4:** (Influence of noisy data in coefficient identification) In the next numerical experiments, we consider the case where the final time measurement $m$ has noise. This is an important subject to study in an inverse problem, since error is always present

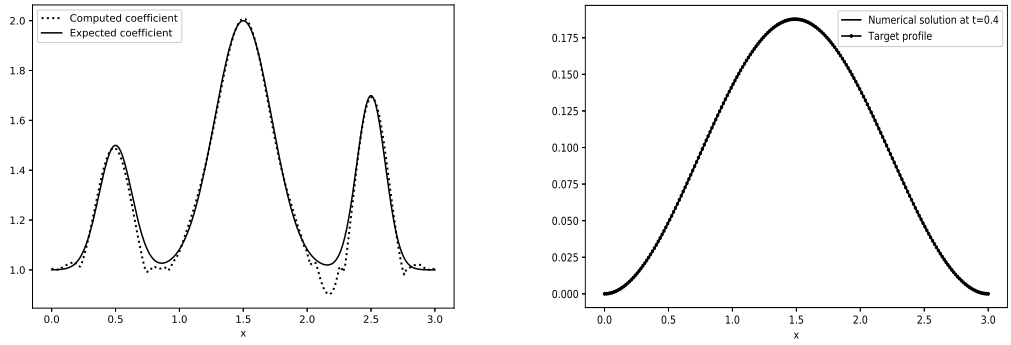


(a) (b)

Figure 2: Experiment 2: (a) Coefficient $\gamma$ (pointed line) computed after 70 iterations of the L-BFGS-B scheme, compared with the expected coefficient (solid line). (b) Final time measurement $m$ (target profile) compared with the numerical solution $u(\cdot, T; \gamma)$ of problem (2) at the final time $T = 0.4$.

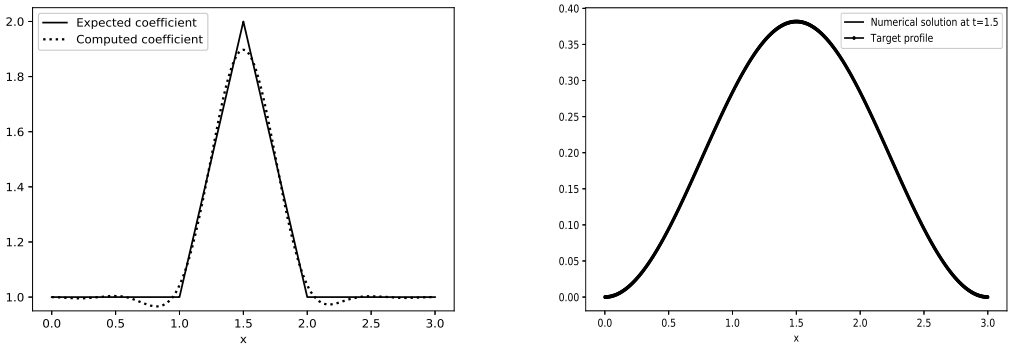


(a) (b)

Figure 3: Experiment 3: (a) Coefficient $\gamma$ (pointed line) computed after 70 iterations of the L-BFGS-B scheme, compared with the expected coefficient (solid line). (b) Final time measurement $m$ (target profile) compared with the numerical solution $u(\cdot, T; \gamma)$ of problem (2) at the final time $T = 1.5$.

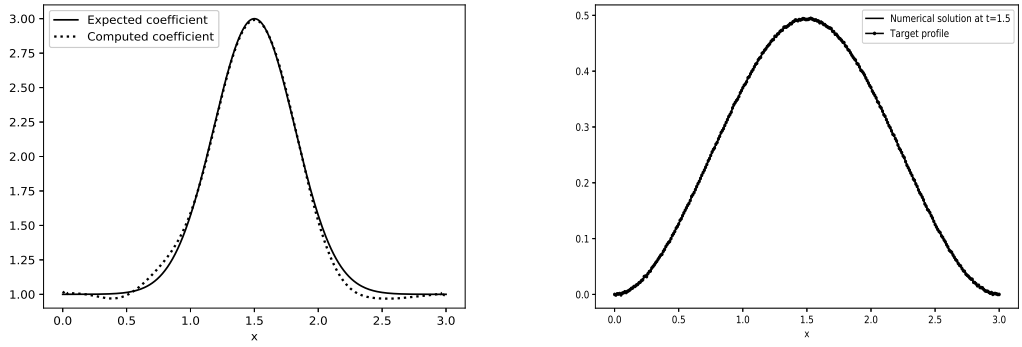


(a) (b)

Figure 4: Experiment 4: (a) Coefficient $\gamma$ (pointed line) computed after 60 iterations of the L-BFGS-B scheme, compared with the expected coefficient (solid line). (b) Final time measurement $m$ (target profile) with Gaussian noise of order $10^{-3}$ compared with the numerical solution $u(\cdot, T; \gamma)$ of problem (2) at the final time $T = 1.5$.

in a measurement, produced for instance by inherently unpredictable fluctuations in the reading of a measurement device or in the experimenter's interpretation of the instrumental reading.

In first place, we consider the same simulation in the experiment 1, but adding Gaussian noise of order $1 \times 10^{-3}$ to the final time measurement $m$. The result of the minimization process after 60 iterations of the L-BFGS-B algorithm applied to the functional $\mathcal{J}_1$ with regularization parameter $\alpha = 10^{-8}$ is presented in Figure 4. The relative difference between exact and computed coefficient in (a) is about $2.7 \times 10^{-2}$ and in (b) the relative difference between the two profiles displayed is of order $6.4 \times 10^{-3}$.

**Experiment set 5:** (Influence of noisy data in coefficient identification). Next, we repeat the simulation in the experiment 2 but adding Gaussian noise of order $1 \times 10^{-3}$ to the final time measurement $m$. Moreover, we use instead the function $\mathcal{J}_2$ as our objective functional with $\alpha = 10^{-6}$. Notice that a larger value of the parameter $\alpha$ than in the experiment 2 was necessary in order to balance the trade-off between data fidelity and solution size of the regularization problem. The result after 60 iterations of the minimization process of this functional is displayed in Figure 6. In (a) the relative difference between exact and computed coefficient is about 0.175, and in (b) the relative error is $2 \times 10^{-2}$. Notice that in this experiment the effect of the noise introduced in the final measurement $m$ is mitigated by the presence of the regularization. Furthermore, although the regularization parameter is very small ($\alpha = 10^{-6}$), it has a significative effect in the inversion process of coefficient $\gamma$. However, the details of the coefficient $\gamma$ are not recovered with the same accuracy as in the absence of noise (compare with the result of Experiment 2 in Figure 2). This is a numerical evidence of the fact that the inverse problem considered here is highly sensitive to changes in the final measurement $m$, and without some regularization term (i.e. $\alpha = 0$) in the objective functional, the minimization process may fail to converge to the expected coefficient $\gamma$, as it can be seen in Figure 5. In this plot the relative difference between the profiles in (a) is about $1.34/2.0 = 0.67$ and in (b) is $3.3 \times 10^{-3}/0.18 \approx 0.018$.

For the experiment in Figure 6, we show in Table 1, the error $e_n = \|\gamma_n - \gamma_{\text{exact}}\|_\infty$ between the computed minimum $\gamma_n$ and exact coefficient $\gamma(x)$ at the step $n$, as well as the corresponding value of the functional $\mathcal{J}_2(\gamma_n)$ as a function of the iterative step $n$. For noisy data, we observe that the error $e_n$ initially decreases as $n$ increases, but when the

| Iteration $n$ | $e_n = \|\gamma_n - \gamma_{\text{exact}}\|_\infty$ | $\mathcal{J}_2(\gamma_n)$ |
|---|---|---|
| 1 | 0.893 | 7.63e-4 |
| 3 | 0.749 | 9.93e-6 |
| 12 | 0.602 | 2.16e-6 |
| 15 | 0.321 | 1.496e-6 |
| 18 | 0.3131 | 1.474e-6 |
| 21 | 0.3284 | 1.4725e-6 |
| 24 | 0.3321 | 1.47113e-6 |
| 33 | 0.3392 | 1.47099e-6 |
| 45 | 0.34339 | 1.47090e-6 |
| 48 | 0.34595 | 1.47088e-6 |
| 51 | 0.34977 | 1.47086184 e-6 |
| 54 | 0.34936 | 1.47086055e-6 |
| 57 | 0.34945 | 1.47086053e-6 |
| 60 | 0.34956 | 1.47086052e-6 |
| 63 | 0.34951 | 1.47086045e-6 |
| 75 | 0.34967 | 1.47085988e-6 |

Table 1: Semi-convergence phenomenon of the L-BFGS-B algorithm. Observe that after iteration 18, the error $e_n$ becomes larger than previous iterations.

algorithm exceeds a certain threshold step, this error becomes larger than the one obtained in previous iterations. Thus, the L-BFGS-B algorithm shows a behaviour often referred to as semi-convergence phenomenon, already observed in the literature [6], [7] for this type of iterative schemes applied to inverse problems. On the other hand, notice that the value of the functional $\mathcal{J}_2(\gamma_n)$ is always decreasing as long as $n$ increases.

**Experiment set 6:** (Influence of noisy data in coefficient identification). Next, we consider the identification of the anti-diffusion coefficient $\gamma$ in the KS equation from the same final measurement $m$ as in the experiment 3 but with Gaussian noise of order $1 \times 10^{-3}$. The parameters are the same as in experiment 3, except that the objective functional $\mathcal{J}_4$ is taken with regularization parameters $\alpha = 3 \times 10^{-6}$ and $\epsilon = 1 \times 10^{-4}$. The result after 70 iterations of the corresponding minimization process is displayed in Figure 7. The relative difference between the profiles in (a) is about $5.8 \times 10^{-2}$, and in (b) is roughly $9.7 \times 10^{-3}$.

The experiments presented above show the robustness and performance of the numerical strategy proposed in the present paper, even when possible errors are present in the final measurement $m$.

**Experiment set 7:** Finally, in Figure 8 we study the behavior of the solution of the optimization problem (4) for the functional $\mathcal{J}_1$, when small disturbances on the final measurement $m$ are introduced. In (a) are displayed the anti-diffusion coefficients $\gamma$ and $\tilde{\gamma}$ corresponding to the measurements $m$ and $\widetilde{m}$ (shown in (b)), respectively, which are separated a distance of $10^{-3}$. In this case, the absolute difference between the anti-diffusion coefficients is around 0.056. The numerical parameters in this experiment were $\Delta t = 0.2/250 \approx 8 \times 10^{-4}$, $N = 200$, $\sigma = 0.4$, and the regularization parameter in the functional $\mathcal{J}_1$ was taken as $\alpha = 10^{-6}$. The final measurement $m(\cdot) = u(\cdot, T; \gamma)$ was obtained by solving the forward problem (64) with the synthetic coefficient $\gamma$ considered in experiment 2 until time $t = T = 0.2$, and the measurement $\widetilde{m}$ was generated by adding Gaussian noise of order $10^{-3}$ to the measurement $m$.

In Figure 9, we repeat the previous simulation but for a smaller final time $T = 0.1$.

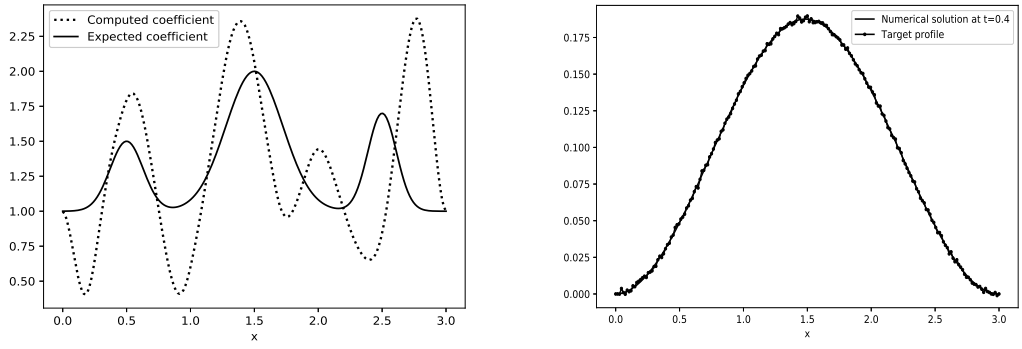


(a) (b)

Figure 5: Experiment 5: Identification of coefficient $\gamma$ without regularization. (a) Coefficient $\gamma$ (pointed line) computed after 60 iterations of the L-BFGS-B scheme, compared with the expected coefficient (solid line). (b) Final time measurement $m$ (target profile) with Gaussian noise of order $10^{-3}$ compared with the numerical solution $u(\cdot, T; \gamma)$ of problem (2) at the final time $T = 0.4$.

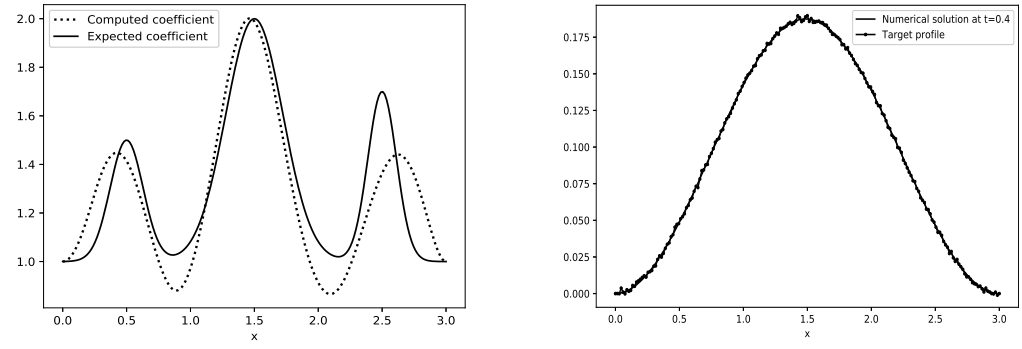


(a) (b)

Figure 6: Experiment 5: (a) Coefficient $\gamma$ (pointed line) computed after 60 iterations of the L-BFGS-B scheme, compared with the expected coefficient (solid line). (b) Final time measurement $m$ (target profile) with Gaussian noise of order $10^{-3}$ compared with the numerical solution $u(\cdot, T; \gamma)$ of problem (2) at the final time $T = 0.4$.

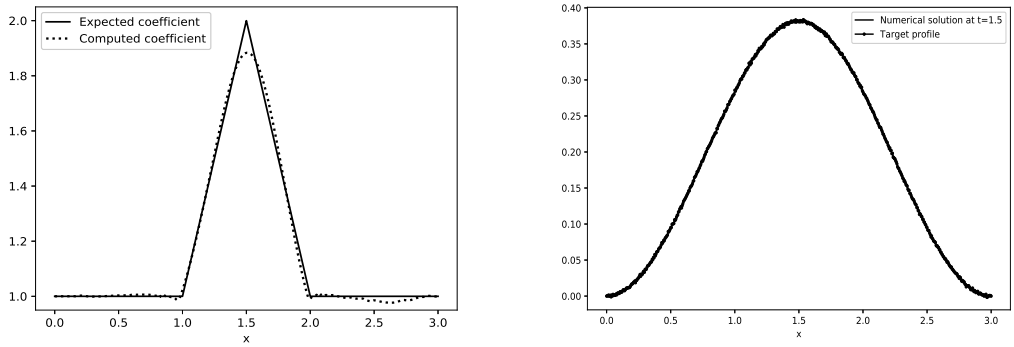


(a) (b)

Figure 7: Experiment 6: (a) Coefficient $\gamma$ (pointed line) computed after 70 iterations of the L-BFGS-B scheme, compared with the expected coefficient (solid line). (b) Final time measurement $m$ (target profile) with Gaussian noise of order $10^{-3}$ compared with the numerical solution $u(\cdot, T; \gamma)$ of problem (2) at the final time $T = 1.5$.

Now the absolute distance between the coefficients $\gamma$ and $\tilde{\gamma}$ computed is about 0.02, which is smaller than in the case of $T = 0.2$. The numerical parameters are the same as in the previous simulation, except that $\Delta t = 0.1/250 \approx 4 \times 10^{-4}$. These numerical experiments are in perfect accordance with Theorem 1.1 on the stability of the solution of the regularized optimization problem (4).

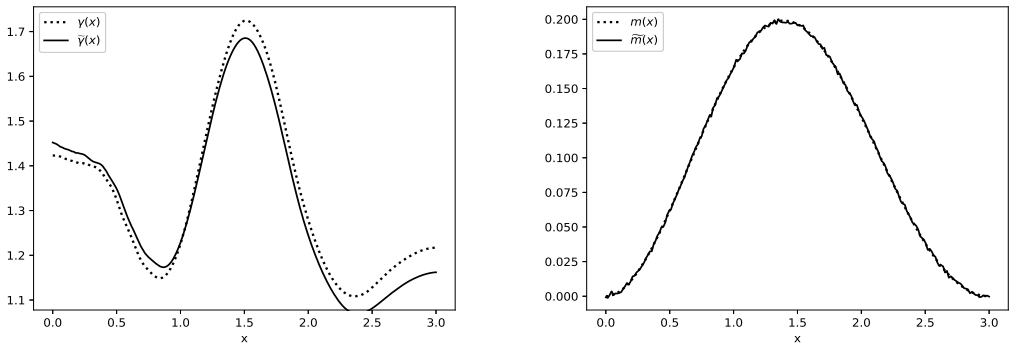


(a) (b)

Figure 8: Experiment 7: (a) Coefficients $\gamma$ and $\tilde{\gamma}$ computed after 70 iterations of the L-BFGS-B scheme corresponding to the final measurements $m$, $\widetilde{m}$ shown in (b). Here the final time is $T = 0.2$.

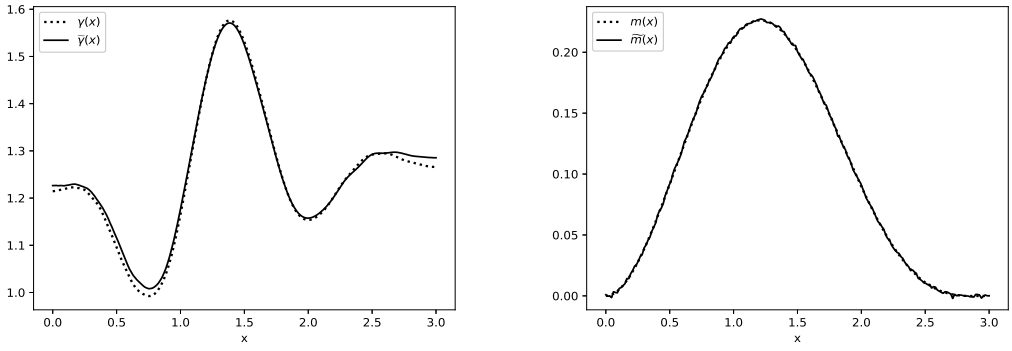


(a) (b)

Figure 9: Experiment 7: (a) Coefficients $\gamma$ and $\tilde{\gamma}$ computed after 70 iterations of the L-BFGS-B scheme corresponding to the measurements $m$, $\widetilde{m}$ shown in (b). Here the final time is $T = 0.1$. Observe that the coefficients $\gamma$, $\tilde{\gamma}$ are closer than those in Figure 8 (a).

# 5 Conclusions

This paper aims to study the inverse problem of recovering the anti-diffusion coefficient in the linear Kuramoto-Sivashinsky equation by means of a final time measurement. The inverse problem was formulated as a non-linear optimization problem, showed a local stability result and developed a numerical scheme for the reconstruction of the parameter, where the forward and adjoint problems for a proper system formulation of the KS equation were approximated by combining a finite element strategy for the discretization of the spatial variable, together with a second-order implicit finite difference method to discretize the temporal variable. With this approach we found better stability properties than with other time stepping schemes. The minimization of the corresponding objective functional was performed by using the iterative L-BFGS-B algorithm from the SciPy-Dolfin-Adjoint libraries implemented in the Python system. We presented several numerical simulations showing the accuracy and robustness of the optimization-based approach considered for different values of the model's parameters, and even in the presence of noise in the final measurement $m$.

As a future work, we are interested in studying the inverse problem of recovering the diffusion coefficient $\sigma = \sigma(x)$ in the KS equation from a final time measurement and in extending the analysis to the nonlinear case. Furthermore, we think that the approach employed in the present paper may be adapted to analyze inverse problems related to other one-dimensional partial differential equations of diffusive or dispersive type.

# References


[1] M.S. Alnæs, *UFL: a finite element form language*, Automated solution of Differential Equations by the Finite Element Method, Springer, 2011.

[2] M.S. Alnæs, J. Blechta, J. Hake, A. Johansson, B. Kehlet, A. Logg, C. Richardson, J. Ring, M.E. Rognes, and G.N. Wells, *The FEniCS Project Version 1.5, Archive of Numerical Software*, **3** (2015).

[3] M.S. Alnæs, A. Logg, K.B. Ølgaard, M.E. Rognes, and G.N. Wells, *Unified form language: a domain-specific language for weak formulations and partial differential equations*, ACM Trans. Math. Software **40** (2014), no. 2, Art. 9, 37. MR 3181899

[4] L. Baudouin, E. Cerpa, E. Crépeau, and A. Mercado, *Lipschitz stability in an inverse problem for the Kuramoto-Sivashinsky equation*, Appl. Anal. **92** (2013), no. 10, 2084–2102. MR 3169149

[5] R.H. Byrd, P. Lu, and J. Nocedal, *A limited memory algorithm for Bound Constrained Optimization*, SIAM J. Sci. Stat. Comput. **16** (1995), no. 5, 1190–1208.

[6] T. Elfving, P.C. Hansen, and T. Nikazad, *Semi-convergence and relaxation parameters for projected sirt algorithms*, SIAM J. Scientific Computing **34** (2012), no. 4, A2000–A2017.

[7] ———, *Semi-convergence properties of kaczmarz's method*, Inverse problems **30** (2014), no. 055007.

[8] L. C. Evans, *Partial differential equations*, Graduate Studies in Mathematics, A.M.S., 1998.

[9] P.E. Farrel, D.A. Ham, S.W. Funke, and M.E. Rognes, *Automated derivation of the adjoint of high-level transient Finite Element Programs*, SIAM J. Sci. Comput. **35** (2013), no. 4, C369–C393.

[10] S.W. Funke and P.E. Farrel, *A framework for automated PDE-constrained optimization*, ArXiv **abs/1302.3894** (2013).

[11] P. Gao, *A new global Carleman estimate for the one-dimensional Kuramoto-Sivashinsky equation and applications to exact controllability to the trajectories and an inverse problem*, Nonlinear Anal. **117** (2015), 133–147. MR 3316610

[12] P. Guzmán, *Lipschitz stability in an inverse problem for the main coefficient of a Kuramoto-Sivashinsky type equation*, J. Math. Anal. Appl. **408** (2013), no. 1, 275–290. MR 3079965

[13] A. Hasanov, *Identification of an unknown source term in a vibrating cantilevered beam from final overdetermination*, Inverse Problems **25** (2009), no. 11, 115015, 19. MR 2558675

[14] R.C. Kirby and A. Logg, *A compiler for variational forms*, ACM Transactions on Mathematical Software **32** (2006), 417–444.

[15] Y. Kuramoto and T. Tsuzuki, *On the formation of dissipative structures in reaction-difussion systems*, Prog. Theor. Phys (1975), no. 54, 687–699.

[16] W.J. Liu and M. Krstić, *Stability enhancement by boundary control in the Kuramoto-Sivashinsky equation*, Nonlinear Anal. **43** (2001), no. 4, Ser. A: Theory Methods, 485–507. MR 1807033

[17] A. Logg, *Automating the Finite Element Method*, Archives of Computational Methods in Engineering **14** (2007), 93–138.

[18] A. Logg, K.A. Mardal, and G.N. Wells, *Automated Solution of Differential Equations by the Finite Element Method*, Springer, 2012.

[19] A. Logg and G.N. Wells, *Dolfin: Automated finite element computing*, ACM Trans. Math. Softw. **37** (2010), no. 2.

[20] A. Logg, G.N. Wells, and J. Hake, *DOLFIN: a C++/Python finite element library*, Automated solution of Differential Equations by the Finite Element Method, A. Logg, K.A. Mardal and G.N. Wells eds., Springer, 2011.

[21] F. Pipicano, J.C. Muñoz, and A. Sosa, *Reconstruction of a space dependent coefficient in a linear Benjamin-Bona-Mahony equation*, Submitted (2019).

[22] E. Rothe, *Zweidimendionale parabolische randwertaufgaben als grenzfall eindimensionaler randwertaufgaben*, Math. Anal. **102** (1930), 650–670.

[23] K. Sakthivel, S. Gnanavel, A. Hasanov, and Raju K. George, *Identification of an unknown coefficient in KdV equation from final time measurement*, J. Inverse Ill-Posed Probl. **24** (2016), no. 4, 469–487. MR 3530560

[24] K. Sakthivel and A. Hasanov, *An inverse problem for the KdV equation with Neumann boundary measured data*, J. Inverse Ill-Posed Probl. **26** (2018), no. 1, 133–151. MR 3757490

[25] SciPy, *https://docs.scipy.org/scipy-1.0.0/reference/generated/scipy.optimize. minimize.html*.

[26] G.I. Sivashinsky, *Nonlinear analysis of hydrodynamic instability in laminar flames i: Derivation of basic equations*, Acta Astronaut. (1977), no. 4, 1177–1206.

[27] C. Zhu, R.H. Byrd, P. Lu, and J. Nocedal, *Algorithm 778: L-bfgs-b: Fortran subroutines for large-scale bound-constrained optimization*, ACM Trans. Math. Softw. **23** (1997), no. 4, 550–560.